Available Online at http://www.journalajst.com

ASIAN JOURNAL OF SCIENCE AND TECHNOLOGY

ISSN: 0976-3376

Asian Journal of Science and Technology
Vol. 11, Issue, 02, pp.10767-10783, February, 2020

RESEARCH ARTICLE

A REVIEW ON SIMULTANEOUS CHEMICAL REACTION AND SEPARATION BY MEMBRANES

Neha Bighane, *Srinivasan Madapusi and Suresh Bhargava

School of Engineering, RMIT University, GPO 2476 Melbourne, VIC 3001, Australia

ARTICLE INFO

Article History:
Received 25th November, 2019
Received in revised form
19th December, 2019
Accepted 07th January, 2020
Published online 28th February, 2020

Key words:
Membranes, Reaction, Membrane Reactor, Catalyst, Ceramic.

ABSTRACT

Conventional membranes provide separation of selective species of molecules from a mixture based on pressure driving force. But sophisticated applications require functional membranes that can provide a basis for a chemical reaction as well as serve their primary purpose of separation based on size and affinity. This paper is a review of membranes that have been applied to challenging applications like simultaneous chemical reaction and separation of products. The scope of this paper is polymeric, metallic, ceramic membranes and pervaporation.

Citation: ***Neha Bighane, Srinivasan Madapusi and Suresh Bhargava*, 2020.** "A review on simultaneous chemical reaction and separation by membranes", *Asian Journal of Science and Technology*, 11, (02), 10767-10783.

INTRODUCTION

Sophisticated separations in pharmaceutics, environmental remediation, resource recovery, etc., require purpose-built separation media. Endowment of functionalities such as specific affinity and reactivity to the media broaden the scope of separations and will facilitate process schemes that are not feasible with currently available technologies. Many chemical reactions occur to a limited extent due to equilibrium constraints; in such cases, removal of one of the products from the reaction mixture will drive the reaction in the forward direction, thereby increase efficiency (completion of reaction) and improving economics of the reaction process. Examples of reactions that can benefit from integration with membranes are esterification, hydrogenation, oxidation, carbonylation, water-gas shift reaction, removal of water from pharmaceutical synthesis process, removal of water from chemical synthesis processes etc. While 'membranes' are robust materials that provide selective permeation of smaller species from a mixture owing to their microscopic structure and properties, 'membrane reactors' are robust materials that can enable chemical reaction and separation of one species from mixture owing to their designed microscopic structure and properties. Basic sciences of membrane reactors are studied through thin films. Ultrathin films have many applications in the fields of microelectronics, tribology, wear resistance, corrosion protection, integrated optics, chemical sensing and bio membranes. These films are typically made using techniques such as solution casting and phase inversion, solution casting and heat-drying, molecular assembly techniques such as Langmuir-Blodgett method, electro-static self assembly, covalent molecular assembly, chemical vapour deposition films and conventional casting techniques like die-pressing and spin-coating. In reality, membranes are scaled-up to real-time processes in the form of high surface-to-volume ratio tubular membranes or hollow fiber membranes. Dense microporous ultrathin films can be coated onto mesoporous tubular or hollow fiber membranes to provide compact modules of membranes or membrane reactors. While there is vast literature on membranes for gas separations and water purification, there is not much information collated about membrane reactors. This paper provides a review on films made to serve two purposes: chemical reaction and separation of product. The scope of this paper is polymeric membranes, polymeric inert reactors, polymeric catalytic reactors, metallic reactors, dense ceramic reactors, porous ceramic reactors and zeolite reactors. The aim of this paper is to fill the gap of a compilation of literature in the field of simultaneous chemical reaction and membrane separation.

Polymeric membrane reactors: Polymers are organic molecules made up of long chains of repeat units. They possess high strength, flexibility and moderate thermal stability depending on their chemical structure. Various types of polymers exist that can be employed for varied applications.

***Corresponding author:* Srinivasan Madapusi**
School of Engineering, RMIT University, GPO 2476 Melbourne, VIC 3001, Australia.

Examples are polysulfone, polyimides, polyamides, polycarbonates etc. Membranes are made of dense entanglements of polymeric chains.

S.R. Lewis and D. Bhattacharya designed a two-layered membrane system for degradation of trichlorophenol (1). In the United States, approximately two-thirds of the over 1,200 most serious hazardous waste sites are contaminated with trichloroethylene (TCE), a potentially carcinogenic compound. TCE and 2,4,6-trichlorophenol (TCP), a carcinogenic and persistent pollutant, represent the large class of chlorinated organics responsible for the contamination of many potential drinking water sources around the world. Various chemical-based treatment technologies also exist for the detoxification of contaminated water sources. A well-known method is via producing free radicals by the reaction of either iron ions (Fe^{+2}/Fe^{+3}) or ferrihydrite/iron oxides with hydrogen peroxide (H_2O_2). The main reaction for the formation of free radicals from Fe^{+2} and H_2O_2 is as follows:

$$Fe^{+2} + H_2O_2 \rightarrow Fe^{+3} + OH^- + OH\bullet \quad (1)$$

where OH• is the hydroxyl radical. Although additional propagation reactions take place during this process, hydroxyl radicals are responsible for the majority of contaminant degradation, which proceeds as follows for a chlorinated organic compound, A:

$$A + OH\bullet \rightarrow I$$

$$I + OH\bullet \rightarrow P + Cl^- \quad (2)$$

where I represents the intermediate compounds formed and P represents the benign oxidized products of the chlorinated organics. To demonstrate the effectiveness of the nanostructured stacked-membrane system, the oxidative degradation of TCP was carried out with a configuration consisting of the Regenerate Cellulose-LayerbyLayer-Graphene Oxide membrane on top of the Poly Vinylidene Fluoride-PolyAcrylicAcid-Fe^{+2}membrane (Fig. 1). The process began by convectively permeating an oxygen-saturated solution of TCP and glucose through the top membrane where GOx converts glucose and oxygen to H_2O_2 and gluconic acid, leaving TCP unaffected. Upon entering the bottom membrane, H_2O_2 reacts with the immobilized Fe^{+2} (reaction 1), generating hydroxyl radicals that react with TCP (reaction 2). Using a constant residence time, the initial conversion of TCP was 100%, but decreased with time, reaching 55–70% after 30 min. This decrease in TCP conversion is characteristic of these PVDF-PAA-Fe+2 membranes as the immobilized Fe^{+2} is converted to Fe^{+3}, reducing the rate of H_2O_2 decomposition and hence free radical production. They demonstrated that through the utilization of this reactive, nanostructured, two-membrane stacked system, harmful organic contaminants can be degraded through the addition of a substrate, glucose, which is enzymatically converted to H_2O_2, thereby eliminating the need for additional chemical reagents. Separation of benzene (Bz) and cyclohexane (Chx) is one of the most challenging processes in the chemical industry. On account of the small difference (only 0.6°C) in volatilities of the two components, conventional distillation processes are not practical. Azeotropic distillation and extractive distillation, on the other hand, although feasible and in use in many industries, are accompanied by high capital and operating costs and also are complex processes in nature. Membrane pervaporation (PV) is

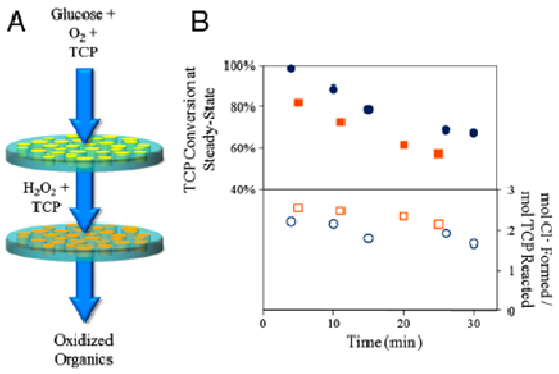

Figure 1. Schematic diagram of stacked membrane reactor for degradation of trichlorophenol [1]

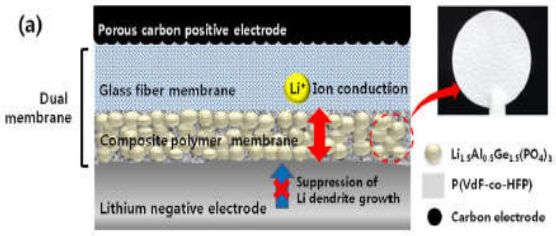

Figure 2. Schematic illustration of lithium-oxygen cell consisting of lithium negative electrode, dual membrane and a porous carbon positive electrode [3]

a viable alternative to the conventional techniques. PV is derived from combining permeation and evaporation, the two mechanisms involved in the process. In a PV process, components of a liquid feed permeate through a membrane and evaporate into the downstream at different rates. Pervaporation is a membrane process in which the feed side is a liquid while the permeate side is a vapour as a result of applying very low downstream pressure like vacuum. There is no chemical reaction involved in pervaporation but there is phase change.

The ideal selectivity is simply the ratio of fluxes of pure substances through the membrane. The actual selectivity of a membrane in a binary system is defined as the ratio of concentrations of components in the permeate to that in the feed. Selectivity of a membrane is strongly influenced by two factors: affinity of the membrane towards one (or more) component(s) of the feed, and ease of diffusion of the permeating molecules through the membrane matrix. Benzene will permeate faster than cyclohexane through a pervaporation membrane since it has a collision diameter of 0.526nm which is smaller than cyclohexane's value of 0.606nm. The best four membranes from a list of reviewed membranes and their corresponding benzene/cyclohexane selectivity are as follows (2):

- MA-G-HEMA which is polymethylacrylate graft 2-hydroxylethyl methacrylate ∞
- Modified Nylon 6 $>10^4$
- CA/PPN which is cellulose acetate /polystyrene diethylphosphonate 40
- DSDA-DDBT which is 3,3',4,4'-diphenilsulphone tetracarboxylicdianhydride/ dimethyl-3,7-diaminobenzothiophene 32

Permeability increases and selectivity decreases sharply, with increasing benzene content of the feed. The decline in the selectivity is explained by the plasticization effect of benzene on the membrane. With increasing benzene content, the membrane is swollen and the relaxed polymer chains allows for enhanced permeation of cyclohexane. Selectivity is high at low temperatures and decreases with increasing T. Flux is low at low temperatures and increases with increase in T. Low fractional free volume and suitable chemical structures were responsible for the high selectivities of the above 4 polymeric material membranes. Selectivity is product of diffusion selectivity and sorption selectivity. In most cases, selectivity of a pervaporation membrane is mainly governed by the sorption component of the selectivity. The domination of sorption selectivity is due to the affinity between the double bonds of benzene molecule and the polar groups of the polymeric membrane. That is, benzene has π electrons, which show stronger affinity to polar molecules. Therefore, a polymer possessing polar groups facilitates the permeation of benzene through the membrane. A proper membrane for Bz/Chx separation must possess both polar groups to facilitate the sorption of benzene and a rigid molecular structure resistive to swelling to retain the membrane's integrity.

The rapid growth of the electric vehicle (EV) market has driven the development of rechargeable batteries with high specific energy and long cycle life. Lithium-ion batteries currently used in EVs have reached practical limits in terms of their energy density.

As a promising alternative to lithium-ion batteries, a non-aqueous lithium-oxygen battery has received great attention due to its high theoretical energy density. Hyun-Sik Woo et.al.demonstrated a two layer composite polymer-glass fiber membrane for enhancing the cycling stability of lithium-oxygen cells by suppressing the lithium dendrite growth and encapsulating the liquid electrolyte effectively in the cell, while maintaining both mechanical stability and interfacial contacts with electrodes during cycling (3). The cell was structured as 1)porous positive carbon electrode in contact with 2)glass fiber membrane in contact with 3)composite polymer membrane in contact with 4)lithium negative electrode.

- The positive electrode was prepared by doctor-blade casting of a slurry composed of 90 wt% Ketjen black EC600JD and 10 wt% poly (vinylidene fluoride) (PVDF, Solvay) binder dispersed in N-methyl pyrrolidone (NMP) on a gas diffusion layer (SGL GROUP, 35 BCE,
- Germany). Disk-shaped electrode having an area of 1.13 cm^2 was punched and vacuum-dried for 12 h at 110°C. glassfiber membrane
- The composite polymer membrane was prepared with Li+ ion-conducting lithium aluminum germanium phosphate (LAGP) particle and poly(vinylidene fluoride-co-hexafluoropropylene) (P(VdF-co-HFP)) copolymer. It was employed with a glass fiber membrane in the form of a dual membrane to fabricate the lithium-oxygen cell.
- Appropriate amounts of synthesized LAGP, P(VdF-co-HFP) (Kynar Flex 2801, Arkema) and dibutyl phthalate (DBP, Sigma-Aldrich) were uniformly mixed in acetone solvent using ball milling machine for 12 h. The resulting solution was then cast using a doctor blade on the glass plate. After evaporation of the acetone solvent for 1 h at room temperature, the cast film was immersed in methyl alcohol for DBP extraction and dried in a vacuum oven at 100 °C for 12 h to eliminate residual solvents. After vacuum drying, the obtained composite polymer membrane was approximately 80-μm thick. The contents of the LAGP in the composite polymer membranes were 50, 60, 70 and 80 wt%.
- The negative electrode was prepared by pressing lithium foil (HonjoMetal Co. Ltd., 200 μm) onto a copper current collector. A Swagelok-type lithium-oxygen cell was fabricated using a lithium negative electrode, a dual membrane (composite polymer membrane and glass fiber membrane) soaked with liquid electrolyte and a carbon positive electrode.

The liquid electrolyte was prepared by dissolving 1.0 M lithium bis(trifluoromethane) sulfonylimide (LiTFSI) in tetra(ethylene glycol) dimethyl ether (TEGDME). The glass fiber membrane prevented nucleophilic attack of superoxide anion radicals on the polymer membrane from the carbon positive electrode. The composite polymer membrane in the dual membrane-based cell prevented the lithium dendrite (Li_2CO_3) growth on the surface of glass fiber membrane from the negative lithium electrode. The composite polymer membrane thus played a role in suppressing lithium dendrite growth. The dual membrane exhibited high ionic conductivity of 8.1×10^{-4} S cm^{-1} at room temperature and exhibited reversible discharge and charge behavior up to 70 cycles without capacity fading.

Based on the obtained results, the dual membrane comprising of composite polymer membrane and glass fiber membrane is proposed as a promising separator for enhancing the cycling stability of lithium-oxygen batteries (3). Tribology is study of friction, wear, abrasion, interfacial friction. Reference (4) by S.R.Puniredd et.al.report the formation of Pd–Pt nanoparticles within a dendrimer-laden ultrathin film matrix immobilized on a solid support and constructed by covalent layer-by-layer (LbL) assembly using supercritical carbon dioxide ($SCCO_2$) as the processing medium. Particle size distribution and composition were controlled by precursor composition. Dendrimers as class of macromolecules are characterized by their globular shape resulting from their perfectly branched architecture and their monodisperse nature. The presence of metal nanoparticles within the dendrimer can markedly improve the nanomechanicalbehavior of nanostructured films. Scott et al. (54) and Ye and Crooks(55) prepared Pt–Pd bimetallic nanoparticles and showed that the reaction rates are enhanced in the presence of the bimetallic nanoparticles compared to dendrimers containing only Pt or only Pd nanoparticles. Supercritical fluids offer potential advantages over conventional solvents for synthesis of nanoparticles. Supercritical carbon dioxide ($SCCO_2$) can be applied as a reaction medium for synthesis of nanoparticles such as Ag, Pt, Pd, Ir, Au, and Ag–Pd from their organo metallic precursors in $SCCO_2$. Additionally, nanoparticles can be formed on solid supports using $SCCO_2$.

Pyromelliticdianhydride (PMDA), second generation polyamidodiaminedendrimer (PAMAM), palladium acetylacetonate ($Pd(acac)_2$), platinum acetylacetonate ($Pt(acac)_2$), iron (III) acetylacetonate ($Fe(acac)_3$), nickel (II) acetylacetonate ($Ni(acac)_2$), boranedimethylamine complex (all from Aldrich), and 3-cyanopropyltrichlorosilane (CPS, Lancaster) were used as received. Trifluoroacetic anhydride (from Aldrich), carbon dioxide (SOXAL Code P40J purified

grade with <20 ppm of H2O), 48% hydrofluoric acid (Sino), acetone, ethanol, *N,N*dimethylacetamide(DMAc), and chloroform (all from Merck) were used directly without further purification. Silicon wafers(Wellbond, Singapore) were 0.6 mm thick, polished on one side and with a natural oxide layer. Quartz slides were purchased from Achema, Singapore.

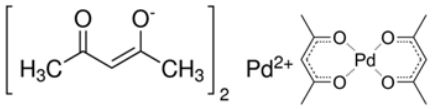

Silicon wafers and quartz slides were modified to form anhydride terminated surfaces by immersion in piranha solution, aminophenyltrimethoxysilane solution and then PMDA solutions.

LbL assembly in $SCCO_2$: The anhydride-derivatized substrates were placed in the column and exposed to a flow of $SCCO_2$ at 40 ◦C and 10 MPa. 100 µL of PAMAM dissolved in DMAc (3 mM) was injected into the $SCCO_2$ stream via a six-way valve (Valco 6CU). PAMAM was performed for 3 h while the flow rate of $SCCO_2$ was maintained at 800 mL/min.

Introduction of metal precursors: Introduction of the precursors in the SCF medium was carried out by injecting 250 µL of 0.15 wt% solution of the precursors (THF for $Pd(acac)_2$, acetone for $Pt(acac)_2$ and methanol for $Fe(acac)_3$ and $Ni(acac)_2$) into the high pressure line at 10 MPa and 40 ◦C via the six-way valve.

Reduction methods: The precursor-laden films were reduced thermally and in $SCCO_2$. Thermal reduction was performed by heating the precursor laden film samples in presence of air at 300 ◦C for 12 h to decompose the acetylacetonate complex. $SCCO_2$ reduction was carried out by injecting 100 µl of dimethylamineborane in ethanol solution (100 mmol/L,0.2 mL) into the high pressure line at 10 MPa and 40 ◦C via the six-way valve. X-ray photoelectron spectroscopy (XPS), UV–Vis absorption spectra, Transmission electron microscopy (TEM), Field emission scanning electron microscopy (FESEM) and Friction test was carried out on a UMT-2 (universal microtribometer). Tribology results are presented in termsof coefficients of friction (COF) that were obtained from the measured normal load and friction force in real time. Presence of $Pd(acac)_2$ in the film is inferred from the observation of strong absorption peaks at 225 nm in the UV–Vis spectra arising from a ligand-to-metal charge transfer (LMCT) transition within the dendrimer.In the case of the Pd–Pt composite (1:1), the LMCT bands due to coordination between the tertiary amines of the dendrimer and the Pt, Pd ions are observed at 225 and 205 nm, and are at the same wavelengths as those observed for the monometallic species.

Table 1. Elemental analysis data on composite thin films [4]

Table 1
XPS elemental analysis of dendrimer-encapsulated Pd–Pt nanoparticles with various Pd–Pt ratios

Pd–Pt ratios (based on injected precursors)	Elemental Pd–Pt ratios measured by XPS
1/1 Pd–Pt	1.03
4/1 Pd–Pt	4.13
10/1 Pd–Pt	11.30
1/4 Pd–Pt	3.11
1/10 Pd–Pt	0.36

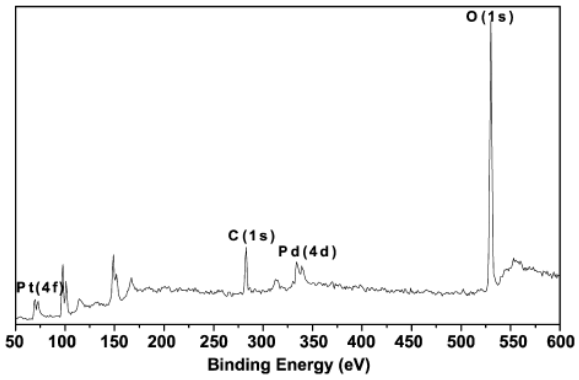

Figure 3. XPS data on composite thin films [4]

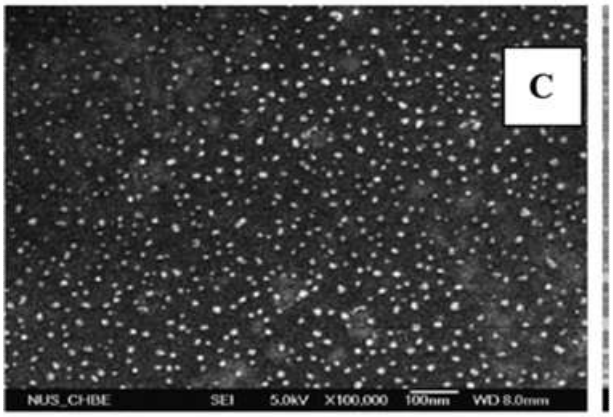

Figure 4. SEM image of 4/1 Pd-Ptnanoaparticles on silicon wafer [4]

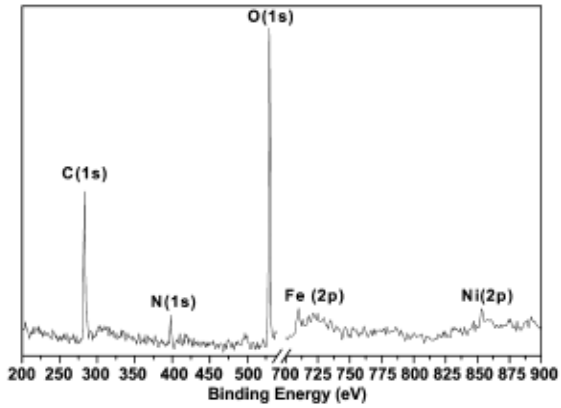

Figure 5. XPS data on composite thin films[4]

XPS wide scans for the nanoparticles of 1/1 Pd–Pt is shown. The sharp signals observed at 73 eV for Pt and 335 eV for Pd indicate that the both Pt and Pd are present. The high quality FESEM image shows the presence of the Pd and Pd–Pt particles in the films. TEM images indicate that the Pd particles are well separated and of fairly uniform size for both thermal and $SCCO_2$ reductions. The particle size of the Pd–Pt nanoparticles from thermal and $SCCO_2$ reductions was 8 ± 2 nm and1.25 ± 0.25 nm, respectively. XPS for 1/1 Fe–Ni ratios, the sharp signals observed at 710 eV for Fe and 855 eV for Ni indicate that the both Fe and Ni are present. From TEM images of 1/1 immobilized Fe–Ni nanoparticles in the dendrimer film for thermal and SCCO2 reductions, the particle sizes from thermal and $SCCO_2$ reductions are 9 ± 2 nm and 1 ±0.2 nm, respectively.

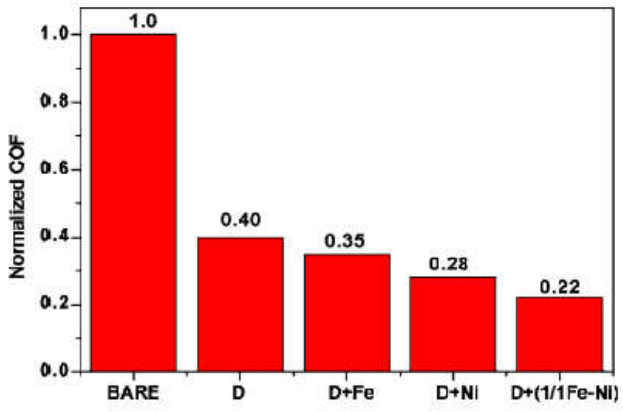

Figure 6. Coefficient of friction tribology data on composite thin films [4]

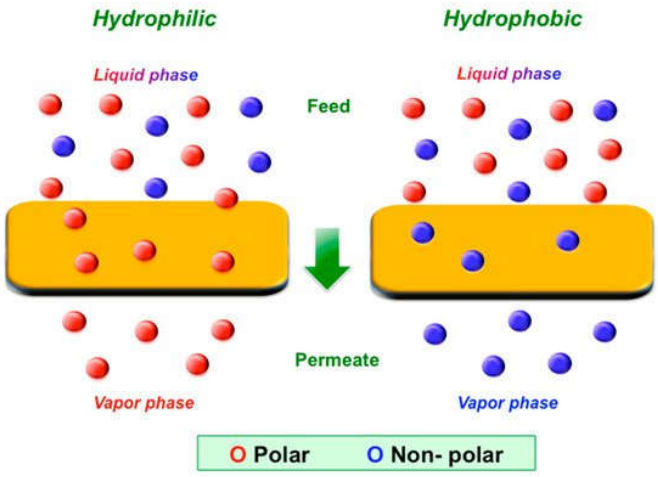

Figure 7. Graphical depiction of the separation mechanisms in pervaporation (PV) for hydrophilic and hydrophobic polymeric membranes towards mixtures of polar and non-polar compounds [6].

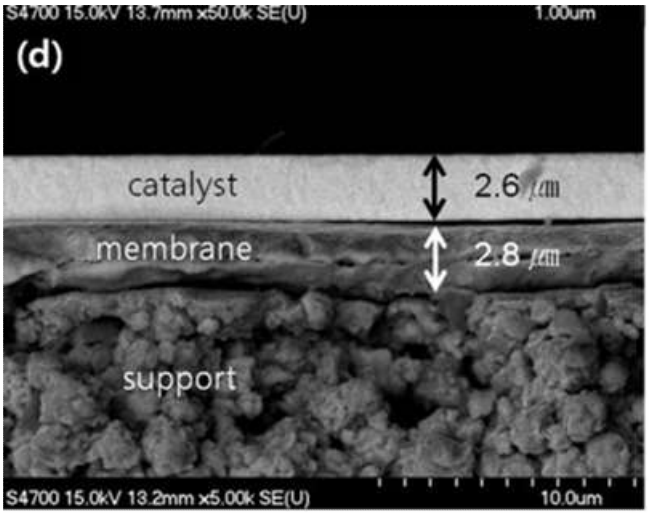

Figure 8. SEM of composite catalyst coated Pd-Au metallic membrane [24]

The decrease in the COF observed after deposition of the dendrimer is due to the multiple amide bonds of the dendrimer which possess friction reduction and anti-wear properties. Deposition of Fe and Ni nanoparticles subsequent to that of the dendrimer layers results in further reduction of the COF.

The COF is again reduced when the combination of Fe and Ni nanoparticles are deposited on the dendrimer surface. Thus, the combination of Fe and Ni nanoparticles within the immobilized dendrimer contribute to enhance the tribological properties when compared to the monometallic (Fe and Ni) particles. Their observation is analogous to the known increase in catalytic efficiency with the use of bimetallic nanoparticles. Thus, this reference from S.Puniredd and M.P.Srinivasan described the use of functional ultrathin films for application to tribology.

Oil–water separation is a worldwide subject because of the increasing demands in numerous applications, such as oilspill accidents, wastewater treatments, and chemical manufacturing. Conventional separation methods, including gravity settlement, gas flotation, coagulation, and electric field or biological treatments, have the limitations of low efficiency, high energy consumption, or multiple operations.In reference (5), a continuous in situ separation of chemical reaction systems based on a special wettable porous polytetrafluoroethylene PTFE membrane was successfully conducted. The membrane possessed (1) an intrinsic (with no modification) special wettability of highly hydrophobic/oleophilic in air and superoleophilic under water and 2) an excellent long-term durability in acidic, alkaline, saline, organic, or heatingenvironments. The in situ separation process exhibited both large separation flux (>3500 L m^{-2} h^{-1}) and high product purity (>99.00%) by continuously filtering synthetic products without interrupting chemical reactions, which is of great significance in industrial fields. Polytetrafluoroethylene (PTFE) is considered the right material due to its excellent properties of chemical inertness, solvent resistance, thermal stability, and low adhesion. Various technologies have been attempted to construct special wettable surfaces with PTFE, such as spray-and-dry method, spinning, RF magnetron sputtering, sol–gel, colloidal deposition, and chemical vapor deposition (CVD). Different from the frequently used coating methods, microporous membrane herein is constructed by directly ablating a piece of PTFE film via a nanosecond pulse CO_2 laser with a fixed wavelength of 1064 nm. A 2 μL oil droplet can spread and permeate through the membrane within 1 s. Contact angles: water in air 114°, oil in air 36°, oil underwater 15.4° (oleophilic). Membrane of four average pore sizes were investigatedM1 (large), M2,M3, M4(small). Due to its importance in synthetic industry, the reaction for producing 2-bromo-2-methylpropane (*tert*-C_4H_9Br) from *tert*-butanol (*tert*-$C_4H_{10}O$) and hydrobromic acid (HBr) is chosen as a typical example. It is one of the most classic nucleophilic substitution reactions to synthesize alkyl halides and the mechanism can be divided into three steps. Sulfuric acid can be added to strongly accelerate the dehydration to generate *tert*-butyl carbocation, which enables the reaction to complete within 1 min. Reactants (*tert*-$C_4H_{10}O$ and HBr) and catalyst (H_2SO_4) are aqueous, while immiscible product (*tert*-C_4H_9Br) is oily. In-air Contact Angles of reactants (≈100°) and product (≈25°) reveal special wettability of a smooth PTFE film toward the chosen reaction systems. Reactants are mixed in the reactor and dyed red by Sudan II (Step 1). When a certain amount of H_2SO_4 is added (Step 2), reaction quickly occurs and an oily product is generated. Then, dyestuff is extracted into the product phase, turning the color of solution into orange (Step 3). After a while, the target product *tert*-C_4H_9Br starts to outflow through the functional membrane, driven by gravity (Step 4).

Table 2. Use of membranes for pervaporation to separate methanol from dimethyl carbonate

Mixture	Aim	Membrane type	Operating conditions	Performance	Reference
Water/methanol/DMC	DMC purification	chitosan	55°C, 2-3mbar	Water flux=0.102kg/m^2.hr Methanol flux=0.250kg/m^2.hr DMC flux=0.011kg/m^2.hr Separation factor =5	[18]
Water-methanol DMC	DMC purification	Crosslinked chitosan	25°C, 2-3 mbar	Total flux=0.180kg/m^2.hr Separation factor =85	[19]
Methanol/ DMC	Methanol removal	PolyAcrylicAcid-PolyVinylAlcohol blend	60°C,2 mbar	Total flux=0.577kg/m^2.hr Separation factor=13	[20]
Methanol/ DMC	Methanol removal	CrosslinkedPolyAcrylicAcid-PolyVinylAlcohol blend	50°C,2 mbar	Total flux=0.040kg/m^2.hr Separation factor=275	[21]
DMC/Methanol	DMC separation	Organophilic ZIF-71 membranes	25 °C	Total flux: 0.271 kg/m^2 h Separation factor: 8.0	[22]

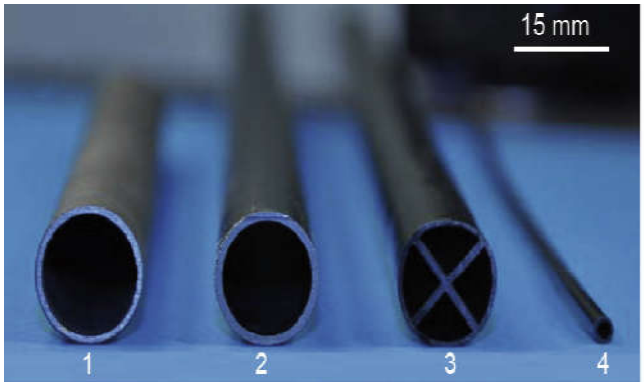

Figure 9.Tubular membranes prepared by isostatic pressing [25]

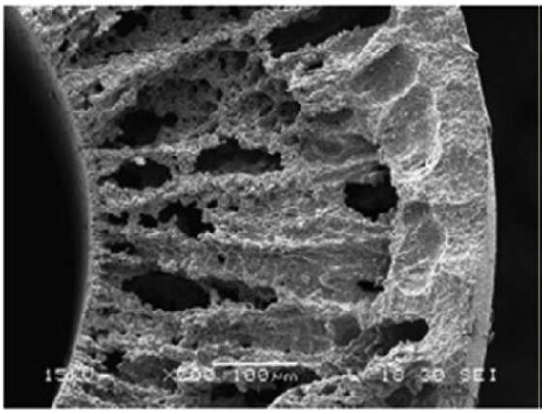

Figure 10.SEM of microstructure of hollow fiber membranes based on mixed conducting materials [37]

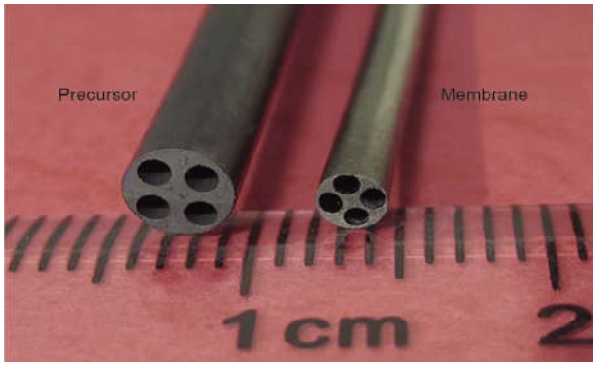

Figure 11. Multichannel hollow fiber ceramic membrane [38]

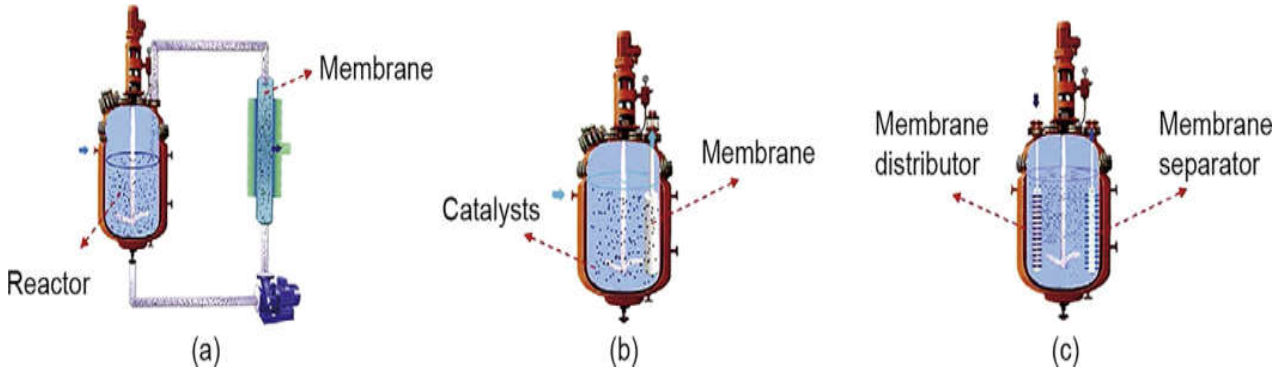

Figure 12. Classic configurations of porous membrane reactors:a) side-stream, b) submerged and c) dual-membrane [25]

If feed of reactants is maintained from the upper catheter, a continuous separation process is underway; if not, a batch one can be conducted (Step 5). When feeding and stirring are stopped, the product can be finally collected (Step 6). It was clearly observed(5) that separation flux increases with the pore sizes of the membranes (3500 ±200, 5100 ±600, 6600 ±700, and 10700 ±400 L m^{-2} h^{-1}, respectively, from M-4 to M-1). The Gas Chromatograph measurements (93.8%, 99.46% , 99.36% , and 99.51% respectively, fromM-1 to M-2 to M-3 to M-4) reflect the high efficiencies of both in situ synthetic reaction and wettability based separation (5). Durability was tested. There was almost no change in the water-in-air CAs (≈130°) after 40 in situ separations. No damage found even after 35 mechanical force cycles. Pressure-driven membrane processes such as microfiltration (MF), ultrafiltration (UF) and nanofiltration (NF) rely on their separation ability on the physical rejection of the species to be separated on the basis of membrane pore size and charge (in the case of NF). The pore size of the membranes can range from 1 μm, for MF membranes, to 2 nm in the case of NF membranes. Dense membranes are operated, on the contrary, in other applications such as pervaporation (PV) and gas separation where the separation of target molecules occurs on the basis of their solubility and diffusivity within the membrane material. Besides these more traditional applications, suitably functionalized membranes can be employed in other innovative fields. The possibility to combine the separation properties of synthetic membranes with chemical transformations operated by specific catalysts has opened up new perspectives in the field of membrane science (6). In all the cases, the membrane always has a separation function.The membrane isolates the reactants from the products of the reaction. This allows us to shift the reaction equilibrium increasing the product yield (this type of MembraneReactor is also known as extractor MR). Moreover, the continuous product removal can avoid the generation of undesired side reactions. The product obtained has generally a high purity and the downstream processing is much easier.

Esterification

Esters may be produced through an esterification reaction by reacting a carboxylic acid with an alcohol in the presence of a mineral acid. Through the use of organophilic or hydrophilic dense membranes, in fact, it is possible to constantly remove the ester or the water increasing considerably the reaction conversion. Souza Figueiredo et al. (7), for instance, studied, in PV, the esterification reaction of acetic acid and ethanol for the production of ethyl acetate considering two different approaches: (1) Reaction and separation conducted in two different and separated steps; (2) reaction and separation occurring in one single step. Amberlyst 35 and 15 were used as catalysts. In the first approach, a Pervap 1000 commercial membrane was used for achieving the separation and the catalyst was dissolved in the feed solution constituted by the alcohol and the carboxylic acid. In the second approach, the catalyst was directly embedded in a polyvinyl alcohol (PVA) matrix used as coating material for the Pervap100 membrane. Both membranes (Pervap 1000 and Pervap 1000 + PVA + catalyst) displayed a hydrophilic character, which made them ideal for the removal of water produced during the esterification reaction.

The catalytic membrane presented an increase up to 60% on ester yield in 8 hours in comparison to the commercial membrane not containing any catalyst, keeping, at the same time, its transport properties (flux of 40 g/m^2 h and an enrichment factor of 17). Therefore, the possibility to directly operate the conversion and the separation in one single step (directly within the membrane) was found to be more advantageous and efficient than running the reaction in two different and separate steps. Zhang et al. (8) reported the application of catalytic membranes in a PV-assisted esterification between acetic acid and *n*-butanol using a three layer membrane made of a porous catalytic top layer, a middle PVA selective dense layer and polyethersulfone (PES) support. Ion-exchange resin of cross-linked styrene-divinyl benzene was used as a catalyst. In batch conditions, pure catalyst beads (not embedded into the membrane) exhibited the best conversion performance (about 68%) while the activity of catalysts loaded into the membrane was just slightly lower (about 65%). The membranes tested in the PV reactor were able to combine the conversion reaction together with the separation of water (by-product of the esterification reaction) reaching an acetic acid conversion of 94.7%, which was about 27% higher in respect to the reaction equilibrium conversion. The removal of water from the reaction medium allowed,in fact, to shift the equilibrium conversion enhancing the formation of the ester. Porous UF polyethersulfone (PES) catalytic membranes were realized by El-Zanati and Abdallah (9) for the esterification between ethyl hexanoic acid with ethanol for the production of ethyl hexanoic ester. Once the PES membrane was produced by a phase inversion technique, the catalyst, consisting of sulfonic groups, was grafted on the membrane surface following a three-step procedure. At the following operating conditions: Temperature of 30 °C, molar ratio of ethanol: carboxylic acid of 5:1 and an internal membrane pore surface of 252,450 cm^2, the maximum conversion rate of 99.7% was obtained.

Hydrogenation

Membranes can offer several advantages in hydrogenation reactions carried out in liquid phase. These types of reactions, in fact, are usually performed at high pressures in order to improve the weak solubility of H_2 in most of the organic solvents. The hydrogenation of furfural to furfuryl alcohol is a relevant industrial conversion for the production of resins. In recent work, Bagnato et al. (10) developed a novel catalytic membrane through the modification of a commercial PES membrane surface with acrylic acid and Ruthenium nanoparticles. When applied for the hydrogenation of furfural, the membranes presented a conversion of 26% after 30 min, a selectivity >99% and a turnover frequency (TOF) of 48,000 h^{-1}. The catalytic membrane, moreover, allowed to operate the conversion under mild conditions with a temperature of 70 °C and a pressure of 7 bar. A series of partial hydrogenation reactions 1,5-cyclooctadiene to cyclooctene, 1-octyne to octene, phenylacetylene to styrene and geraniol to citronellol was studied by Schmidt et al. (11) using a porous polyacrylic acid (PAA) membrane and immobilized Palladium particles as catalysts. The selectivity of conversion reactions operated by the membrane reactor was compared to the fixed bed reactor (FBR) and slurry reactor (SR) where no membranes were used. The membrane reactor showed in all cases better results in terms of selectivity in comparison to the other two approaches considered.

In particular, for phenylacetylene and 1,5-cyclooctadiene a selectivity of 90 was obtained, while for 1-octyne and geraniol a selectivity of 93 and 50, respectively, were achieved.

Oxidation

The preferred way to produce maleic anhydride (MA) is currently based on the oxidation of butane, which replaced the previous synthetic route based on the partial oxidation of benzene. Butane in comparison to benzene presents some advantages like lower cost, lower toxicity and higher availability. However, the high flammability of butane limits the reaction process imposing to work at butane concentrations not higher than 2 vol %. In the study of Cruz-Lòpez et al. (12), employment of a catalytic membrane reactorfacilitated the oxidation reaction to be carried out at higher butane concentration using a MFI/alumina membrane. The distribution of oxygen, used as a reactant, through the membrane allowed, in fact, the lowering of its concentration outside the flammability range. The reaction was catalyzed by a cobalt doped V/P/O (VPO) catalyst. A high Maleic Anhydride selectivity conversion level of 75% was obtained with productivity three times higher (435 mol m^{-3} h^{-1}) than conventional reactors. The partial oxidation of methane is used to convert CH_4 to syngas (CO and H_2). The development of plants, at the commercial level, able to operate this conversion encountered some difficulties mainly because the reaction is partially exothermic creating local hot spot problems. Membrane reactor can overcome this limitation controlling the reaction stoichiometry and the interaction of reactants. Knipe and Lin (13), for instance, operated the partial oxidation reaction of methane using a dense SrCoFeOx membrane using different catalysts (catalyst support γ-Al_2O_3, $La_{0.6}Sr_{0.4}Co_{0.8}Fe_{0.2}O_3$-δ, Ni/$\gamma$-$Al_2O_3$). The membrane reactor with Ni/γ-Al_2O_3 catalyst displayed the best performance in terms of CH_4 conversion of 90% at 900 °C, high CO selectivity and moderate O_2 flux of about 2.4 mL/cm^2 min. In comparison, the blank membrane prepared with Al_2O_3, presented, under the same operative conditions, a CH_4 conversion of about 19%, CO selectivity of about 58 and an O_2 flux of about 0.71 mL/cm^2 min.

Carbonylation Reactions: The most promising routes of synthesis of dimethyl carbonate (DMC) are based on the oxidative carbonylation of methanol and the direct synthesis of DMC from CO_2 and methanol (6). Li and Zhong (14) evaluated the use of three different supported membranes with copper catalyst supported on a$MgO–SiO_2$ substrate modified by KF for the synthesis of DMC. The membranes used for studying the conversion performance were represented by a mesoporous silica membrane supported on a TiO_2/K-M ceramic tube (membrane S), a polyimide-silica hybrid membrane supported on a TiO_2/K-M ceramic tube (membrane PS) and a polyimide–titania hybrid membrane supported on a TiO_2/K-M ceramic tube (membrane PT). The results were compared with a traditional conversion catalytic reaction (CCR). In CCR, the reaction of CO_2 with methanol leads to the production of DMC and H_2O in the primary reaction and to the formation of HCHO and CO in the secondary side reaction. The conversion of methanol and the selectivity to DMC measured were of 6.55% and 90%, respectively. Under the same operative conditions, all the three membranes displayed better performance in terms of conversion of methanol (8.1, 9.2 and 8.9 for the S, PS and PT membranes, respectively) and of selectivity to DMC (91.4, 96 and 93.3 for the S, PS and PT membranes, respectively). Improvements in performance were attributed to the hydrophilic nature of the membranes, which allowed a favorable permeation of the by-product H_2O shifting the equilibrium towards the formation of the product. Even if the improvements were modest, it was demonstrated in this work, for the first time that the introduction of membranes for the production of DMC can lead to an enhancement in catalytic reaction performance.

Yamanaka et al. (15) studied the DMC production through the electrochemical carbonylation of methanol and CO. A polytetrafluoroethylene (PTFE) porous membrane containing a Pd based catalyst acting as an anode and a PTFE membrane containing Pt black and acting as a cathode, were assembled into an electrolysis cell. The space between the two porous PTFE membranes was filled with a solution containing methanol and an electrolyte while a CO gas was fed through the anode side. The screening of different electrolytes showed that $NaClO_4$ (sodium perchlorate) was the best one in terms of DMC production at 298 K and an electrolysis voltage of 3.5 V. Dimethyl oxalate (DMO) was found to be the major by-product produced during the synthesis and its concentration increased as the formation of DMC increased. One of the advantages of using a three-phase boundary electrolysis method was the possibility of supplying more CO (higher partial pressure) promoting the selective carbonylation of DMC. Increasing the CO partial pressure (up to 100 kPa), in fact, the formation rate of DMC increased (up to 80 μmol cm^{-2} h^{-1} at 100 kPa) while the formation rate of the by-product DMO decreased (about 10 μmol cm^{-2} h^{-1} at 100 kPa). This three-phase boundary electrolysis method allowed the production of DMC with the following maxima values: TON (Pd) of 192 h^{-1}, CO selectivity of 82% and DMC selectivity of 88%. Generally, Pervaporation is able to separate azeotropic, close boiling-point, diluted and thermally unstable liquid mixtures, where a phase change from liquid to vapor takes place. PV has become attractive for scientists because of its several advantages, such as low energy consumption, lack of any solvent requirements and the fact that it is not limited by the vapor-liquid equilibrium. In principle, the liquid feed mixture is in direct contact with the “selective” side of the PV membrane, while the permeate (the stream collected at the other side of the membrane) is in the vapor phase maintained under vacuum, which gets enriched with the permeating species having a higher affinity for the membrane(16).

DMC has been the most explored chemical in this field. The importance of DMC deals with its use as a green chemical agent. DMC is indeed considered as a potential candidate for the replacement of methyl-*tert*-butyl ether (MTBE) as an oxygenated fuel additive of gasoline or diesel oil. These purposes have rapidly promoted the increasing of its application in the last years. The synthesis of DMC is typically carried by means of several routes, such as phosgenation of methanol (MeOH), urea methanolysis, transesterification of cyclic carbonates, direct reaction of CO_2 with MeOH and, of course, oxidative carbonylation of MeOH. However, in all aforementioned methodologies, DMC and MeOH form a minimum boiling azeotrope containing almost 70 wt % methanol and traces of other polar compounds (e.g., water). The conventional distillation (e.g., extractive distillation and pressure-swing distillation) has been the primary technology used for the purification/separation of DMC (17).

Today, according to the several drawbacks of distillation (e.g., high-energy demand), PV has started to be proposed for the purification of DMC. At this point, PV membranes are primarily tested for such MeOH–DMC separation. Since MeOH is a more polar compound and has a smaller molecular size than DMC, the common strategy for the separation of these mixtures, is based on the use of hydrophilic polymers. Table 2 lists the performance of some pervaporation membranes for MeOH/DMC separation (6). In PVA-PAA crosslinked membranes, the study reported that the separation factors decreased but the fluxes increased with increasing MeOH concentration in feed from 40 to 70 wt %. This result can be explained considering the MeOH plasticization effect toward the membrane. As the MeOH concentration in the feed increased, the membrane becomes more swollen because of a stronger affinity with it. Consequently, the polymeric chains tend to be more flexible and the energy required for diffusive transport is less, resulting in a flux increase.

Challenges for polymeric membranes: 1) Polymeric membranes undergo fouling or scaling upon repeated exposure to feed solutions with or without chemical reactions. When there is a scaling issue, the membrane must be flushed with plain water to remove the contaminants from its pores. After this, the membrane must be subject to vacuum to dry its pores.

- Under high pressure conditions (>150-300psia), polymeric membranes swell (indicated by higher than normal permeability) which is called plasticization and leads to decrease in selectivity.
- Polymeric membranes have aging and typically have a shelf life of 6-10months.
- The sealing epoxy must be compatible with the polymer material for making modules.

Glass membrane: In reference (23), Sun and Khang's research demonstrated the possibility of achieving conversions above the original equilibrium conversion based on the feed conditions by combining the selective separation effect of a membrane and the catalytic function of transition metals. A catalytic membrane reactor, containing a tubular Vycor glass membrane which was impregnated with a platinum catalyst, was studied with the model reaction of cyclohexane dehydrogenation. The equilibrium shift was significant for the operation with high space time. A number of investigations have concentrated on the membrane reactor built with a microporous Vycor glass membrane (average pore diameter of about 40Å, surface area of about 200-250 m^2/g, porosity of about 0.28, and density of about 1450-1500 kg/m^3).

All of these researchers employed a tubular Vycor glass membrane reactor with a bed of catalyst on the feed side (upstream or reject stream). Experiments and simulations in their studies showed that the chemical equilibrium shift could be favorably achieved because the hydrogen (one of the products) was preferentially removed from the reaction zone. However, the Vycor glass membrane itself has a large surface area (200 m^2/g), and for this reason, it is possible to use the membrane also as a catalyst carrier. It was interesting, therefore, if the membrane was impregnated with catalytic transition metals so that the catalytically impregnated membrane would perform a dual function of chemical reaction and selective separation. The platinum-catalyzed dehydrogenation of cyclohexane was used as a model reaction.

$$C_6H_{12} \leftrightarrow C_6H_6 + 3H_2 \quad (3)$$

An annular catalytic membrane reactor was designed. The feed-side (upstream pressure,) P_f, was higher than the permeate-side (downstream) pressure, Pp. The total molar flow rate and the composition of each input stream was maintained constant during the operation.
The rate constant was derived as

$$k = 3.754 \times 10^{11} \exp\left(\frac{-1.598 \times 10^5}{RT}\right) \quad kmol/(m^3 \cdot s \cdot kPa)$$

87-92% conversion in catalytic membrane reactor was achieved (23).

Metallic membranes: Metallic membrane reactors are fabricated from metals like platinum, palladium, iron, nickel, gold, silver etc. As a novel approach to simultaneous water-gas shift (WGS) reaction and separation for the production of hydrogen, a bi-functional membrane was successfully prepared using a simple coating method in reference (24). The catalyst materials, Pt and CeO_2, were directly coated over the surface of Pd-Au dense membrane. The coated catalyst layer did not significantly affect the hydrogen permeance of the bare membrane. As a result of WGS reaction ($CO+H_2O \rightarrow CO_2+H_2$) within the novel membrane reactor at 380°C, the CO conversion was 2 times higher than that of no hydrogen separation (24). For instance, a Pd-Ag membrane reactor was prepared for pure hydrogen production via WGS reaction where the Pd-Ag membrane tube was surrounded by a catalyst bed in the shell side. The achieved CO conversion of 90% was 3-4 times higher than that of a traditional reactor.In this reactor (a) which consists of a WGS catalyst bed and membrane, the following steps are utilized; (1) adsorption of reactants (CO and steam) over the surface of catalysts, (2) catalytic reaction, (3) desorption of products (H_2, CO_2, etc.) from the catalysts, (4) bulk diffusion of hydrogen to the surface of the membrane, (5) dissociative adsorption of hydrogento H atoms at the surface of Pd film, (6) diffusion of protons into the Pd-based layer, and (7) associative desorption of the H atoms.

The coin-shaped, 50 mm, Pd-Au membrane was prepared using the DC power magnetron sputtering system with a plasma cleaning system (Korea Vacuum Tech., LTD, KVS-4004L) over a compressed and polished nickel metal support. Zirconia was used as an interdiffusion barrier between Pd-based layer and nickel support. After the Pd-Au deposition, the membrane was sintered at 700°C for 2 h (24). In order to enhance the selectivity of the ultra-thin membrane, the prepared membrane was finally polished with alumina slurry using an automatic polishing machine(GNP Tech., Poly-300).
The coin-shaped bi-functional membrane was prepared by coating catalyst materials over the surface of the prepared Pd-Au membrane. The Pt-CeO_2 catalyst, a representative. WGS catalyst, was coated by the co-sputtering method with Platinum and Cerium Oxide targets with the rotation of a sample holder at room temperature. A DC and RF power supply provided the power needed to generation plasma for the deposition Pt and CeO_2. After the Pt-CeO_2 deposition, it was stabilized at 400°C for 48 h under the H_2 atmosphere. The thickness of the Pd-based membrane film, supported by porous nickel, was about 2.8 μm.

The depth of catalyst layer was about 2.6 μm. Hydrogen permeance flux varied as 0.6 power of pressure difference in bare membrane. Hydrogen flux varied slightly in bi-functional membrane as a function of transmembrane pressure and temperature. Hydrogen flow rate decreased as percentage of CO or steam increased due to competitive adsorption. The flow rate of feed was 200 mL/min and the calculated gas-hourly space velocity (GHSV) was extremely high (2,200,000 h^{-1}) due to the very thin catalyst layer, 2.6 μm. The reaction was performed at 380°C at which equilibrium conversion is calculated to be 96.97%. At pressure difference of 10bar, CO conversion was 30% and hydrogen permeate flow rate was 5ml/min (24). In reference (53), Emma Palo et.al. describe three pilot plants tests based on palladium membranes. On the basis of their flexibility, membrane reactors can be employed in a wide range of applications where energy saving and the enhancement of performance in terms of reactants conversion and products selectivity can lead to improved economics. Among the different membrane reactors reported in the scientific literature, the palladium-based ones are the most commonly used when hydrogen is separated as the product in permeate stream. In palladium membranes, the permeance follows Sievert's law. Several application areas of Pd-based membrane reactors have been considered by KT—Kinetics Technology (KT):

(i) pure hydrogen production; (ii) gas-to-liquid (GTL) processes; (iii) propylene production. Natural gas (NG) steam reforming is the most widely used hydrogen production process. Currently, around 50% of the worldwide hydrogen yearly production results from this technology. The main reaction occurring in NG steam reforming is endothermic to produce syngas ($CH_4 + H_2O \rightarrow CO + 3H_2$) and it is limited by chemical equilibrium, thereby significant hydrogen yields are achieved only with operation at high temperatures (850–900 °C). As a consequence, a portion of methane feedstock must be burned in furnaces in order to sustain the reaction heat duty. This can be responsible for a reduction of the overall process efficiency, an increase of greenhouse gas (GHG) emissions and a dependence of the hydrogen production cost on the natural gas cost. Accordingly, the coupling of the reaction unit with hydrogen-selective membranes can represent a promising way to enhance hydrogen yield at lower temperatures, since the continuous selective removal of hydrogen from the reaction environment allows to maintain the gas mixture composition far from equilibrium, so that equilibrium conditions are not achieved (Le-Chatelier's principle) and the endothermic reaction can be carried out at a lower temperature.

- The lower thermal duty could also allow the operation of the membrane reformer with a cleaner energy source or with waste heat available from another process, instead of the high-temperature flue gases used in the furnace.
- Moreover, the lower operation temperature allows to use cheaper steel alloys for the fabrication of the reforming tube instead of the expensive materials currently used to withstand the high operating temperatures of conventional steam reforming plants.

There is a significant incentive for developing new technologies to decrease the capital and operating cost of syngas production units. Propylene is one of the most important derivatives in the petrochemical industry, after ethylene. Worldwide, propylene is mostly produced as a co-product in steam crackers (>55%) or as by-product in Fluid Catalytic Cracking (FCC) units (around 35%). However, the high reaction temperatures of such processes, as well as the high instability of hydrocarbons, lead to formation of coke and the occurrence of side reactions that significantly impact propylene yield. In order to meet the increase in the market demand, being estimated as 5% per year, several "on-purpose" technologies have been proposed as propylene sources, such as propane dehydrogenation (PDH), methanol-to-propylene (MTP) conversion, and olefin metathesis. It is widely recognized that, in the longer term, "on-purpose" propylene production technologies will be able to stabilize the supply–demand balance.

PDH ($C_3H_8 \rightarrow C_3H_6 + H_2$) is a highly endothermic reaction, accordingly favored at high temperatures of operation. In these operating conditions, other side reactions usually can be observed responsible for the production of lighter hydrocarbons or coke deposited on the catalyst, thereby forcing to carry out a periodic catalyst regeneration in order to recover its activity after deactivation. The two targets of decreased coke formation and increased propylene yield could be in principle achieved by integrating a low-temperature dehydrogenation reaction step with a H_2-selective membrane. Ideally, a membrane reactor would i) enable the operation at a lower temperature, (ii) providing the high conversion and selectivity and (iii) reducing frequent regeneration cycles. Pd-based membranes appear as the most promising solution for the integration with the PDH reaction, owing to their significant selectivity/flux ratio and to the conventional operating temperature (400–500°C) that is aligned with the PDH reaction operating conditions. A selective membrane can be integrated with the reaction environment in two different configurations, with different benefits and drawbacks: (i) the selective membrane is in direct contact with the reaction environment/catalyst, and the reaction product is continuously removed simultaneous to its production (Integrated Membrane Reactor (IMR) also called closed architecture) OR (ii) the selective membrane is not in direct contact with the reaction environment/catalyst but installed outside the reactor and followed downstream by another reaction unit, where the overcoming of chemical equilibrium is observed (Staged Membrane Reactor (SMR), or Reactor and Membrane Module (RMM) also called open architecture).

Pure Hydrogen Production: For the pure hydrogen production case, both architectures were studied. The open architecture was tested at pilot level and at a capacity of 20 Nm^3/h of pure hydrogen (facility available at Chieti Scalo, Italy, Italian FISR project). The plant was characterized by two-stage reformers and two membrane modules operated in the temperature range 550–650 °C and 400–450 °C, respectively. Natural gas, available at 12 barg, was subjected to desulphurization and then mixed with the process steam. Each reforming module is characterized by two main sections:(i) a radiant tube, loaded with the catalyst, and (ii) a convection section. The syngas produced in the first reformer R-01 was cooled down to the temperature suitable for membrane operation and fed to the first separation module M01A/B (0.4 and 0.6 m^2 respectively). The retentate was sent to the second reformer R-02, at the outlet of which a mixture with an increased amount of H_2 in consequence of the higher feed conversion was produced. The syngas from the second

reformer stage was cooled down from 650°C to the temperature suitable for membrane operation and routed to the second separation module (M-02, 0.13 m^2). H_2 recovered from both membrane modules was collected and routed to the final cooling and condensate separation. Permeance was 32-35 Normal $m^3/hm^2.bar^{0.5}$ at 400°C and hydrogen recovery was about 36%. Hydrogen purity of at least 99.9% mol was detected for all membranes. With the number of reaction stages up to six, for example, feed conversion increased up to 70% and 90% at a reformer outlet temperature of 650 °C and 600 °C, respectively. The closed architecture was tested at pilot level plant of capacity of 3 Nm^3/h of pure hydrogen (facility available at ENEA Casaccia, Italy, EUComethy project). The plant architecture is based on a first pre-reformer stage (R-01) followed by an integrated membrane reactor (R-02). R-01 is organized as a shell-and-tube configuration, where the molten salts mixture flows in the shell side supplying reaction heat and the catalyst is installed inside the tubes. R-02 is also arranged in a shell-and-tube configuration, with the molten salts flowing on the shell side. Catalyst and membrane are arranged according to a tube-in-tube configuration, with the catalyst in the annular section around the membranes tube. The nickel noble metal-based catalysts deposited on silicon carbide foam were shaped in the form of a cylinder and an annular cylinder for R-01 and R-02, respectively. The catalysts were prepared at the ProCeed Lab of the University of Salerno. A total of 10 Pd-based membranes on ceramic supports were arranged in R-02, developing an overall area of about 0.35 m^2. Each membrane had an outside diameter of 14 mm and a length of 80 cm. To improve the separation efficiency, superheated steam was employed as sweep gas in a countercurrent configuration. Permeance was 10-15 $Nm^3/hm^2.bar^{0.5}$at 400-450°C. The experimental results showed that, under a molar sweep gas/feed ratio equal to 1.5, the feed conversion increased up to 135–150% with respect to an operating condition without sweep gas.

Synthetic fuel production: The overall concept was tested in open architecture at pilot level of a capacity of 20 Nm^3/h of pure hydrogen (facility available at Chieti Scalo, Italy, EU NEXT-GTL project). After desulphurization, the natural gas was mixed with the process steam and preheated in the convective section of the reformer. The preheated steam was further routed to the reforming reactor operated at an outlet temperature of 550–600 °C. The syngas produced was cooled at a temperature in the range of 450–480°C before entering the first Pd-based membrane module M-01, where a permeate and a retentate stream were produced. The retentate mainly CO, poor in hydrogen, was routed to the CPO (catalytic partial oxidation) reactor and mixed inside the reactor with a stream of pure oxygen from gas cylinders. The hot syngas available at the outlet of the CPO reactor was cooled down to 450–480°C in a gas–gas heat exchanger and routed to the second Pd-based membrane separator M-02 for a further hydrogen recovery step. Structured catalysts in the forms of honeycomb monolith and pellets, both based on noble metals, were used in the CPO reactor. When operating the reformer at an outlet temperature of 590 °C, P = 11 atm, a hydrogen. Recovery Factor (HRF) of 45% and with a ratio $O_2/(CO + CH_4)$ at the inlet of the CPO reactor of 0.16 was attained. A significant reduction in the hydrogen content was observed in the retentate stream due to hydrogen recovery carried out by the first-stage membrane, whereas the concentration of other products increased. In addition, the performance of the membrane system remained stable for 100hr continuous operation. Looking at the economics of the novel process for syngas production, it can be observed that the solution consisting of the CPO reactor integrated with the reformer and the membrane enables a reduction in oxygen consumption, since a portion of feed conversion is achieved in the upstream reformer stage. The removal of hydrogen in the first membrane module has the double role to favour both reactions of partial oxidation of methane and steam reforming inside the CPO reactor. It is possible to observe that, if a total feed conversion of 40% is taken into account, the integrated architecture allows to reduce the oxygen consumption over 50%. This can be translated into a lower operating temperature for the CPO section with a difference in the outlet gas composition. The achieved reduction of oxygen consumption enables a reduction of about 10% in the variable operating cost.

Propylene production: The overall concept was tested in open architecture at pilot level of capacity of 0.05 kg/h of propylene (facility available at the University of Salerno, Italy, EU CARENA project).The experimental apparatus consisted of two tubular catalytic reactors (R-101 and R-102)and, between them, a selective separation unit (membrane, M-101 in “open architecture” of the membrane-based process. The catalytic units consist of a catalytic reactor of tubular shape and made of AISI 310 stainless steel (SS); the reactor was loaded with a platinum–tin-based catalyst. Overall permeation surface was 0.01 m^2. It can be observed that, with a membrane permeance of 40 $Nm^3/(m^2hbar^{0.5})$ at 550°C, it was possible to increase the propane conversion to 35%.The improvement of such performance became 48% when the membrane permeance was increased up to 80 $Nm^3/(m^2hbar^{0.5})$. Presence of membrane decreased the operating temperature which in turn reduced amount of coke formation. It is much more desirable to limit the membrane operation at temperatures not higher than 400 °C, after a decline in hydrogen flux is observed, owing to the tendency of propylene to form oligomers and ring structures on the membrane that can reduce the performance. The overall results reported up to now, show the effective applicability of Pd-based membrane reactors in a very large number of chemical processes. The actual industrial implementation is strongly related to the possibility of having a stable membrane performance for a long period (at least about 10,000 h) and a cheap cost (53).

Ceramic membranes: Catalytic membrane reactors (CMRs), which synergistically carry out reactions and separations, are expected to become a green and sustainable technology in chemical engineering. The use of ceramic membranes in CMRs is being widely considered because it permits reactions and separations to be carried out under harsh conditions in terms of both temperature and the chemical environment. Reference (25) presents the two most important types of CMRs: those based on dense mixed-conducting membranes for gas separation, and those based on porous ceramic membranes for heterogeneous catalytic processes. There is a discussion on:

- Configuration of membrane reactors
- Design and optimization for model reactions
- Challenges and difficulties in industrializing membrane reactors

Inorganic membranes, which are typically ceramic membranes (e.g., metal oxides), have obvious advantages in terms of chemical and thermal stability, fouling resistance, mechanical strength, and lifetime compared with polymeric membranes. One type of CMR is based on the dense ceramic membrane, which is a type of gas-separation membrane. Perovskite-type mixed ionic–electronic conducting membranes are one of the most studied dense ceramic membranes. These membranes have a generic composition of ABO_3, where A is a lanthanide, an alkaline-earth element, or a mixture of the two, while B is normally a transition element. The properties of perovskite-type membranes are closely associated with the A- and B-site cations and their composition. At an elevated temperature (normally higher than 700°C), these membranes simultaneously exhibit oxygen ionic and electronic conductivities, and have a theoretical 100% selectivity to oxygen. The most attractive qualities of these membranes are their high oxygen flux (and permselectivity) and high catalytic activity. Certain important gas-phase catalytic processes, such as the utilization of natural gas, the production of hydrogen, and the treatment of greenhouse gases, can be carried out in CMRs based on perovskite-type membranes (26-33). The other type of CMRs is based on a porous ceramic membrane and is mainly used for heterogeneous catalytic processes. In heterogeneous catalytic reactions in the presence of suspended ultrafine or nano-sized catalysts, a membrane with an appropriate pore size can effectively separate the catalysts from the reaction slurry. 'Expensive catalyst' separation and reactant distribution can be simultaneously achieved with an appropriate reactor configuration design, which can prevent decrease in overall selectivity and yield of process.

***Dense ceramic membrane reactors*:** There are three main types of ceramic membrane architectures: disk-like (or planar) membranes, tubular membranes and hollow fiber (HF) membranes. Disk-like membranes with a limited membrane area are usually used for kinetics studies because of their simple fabrication procedure. A planar membrane can be fabricated on a very large scale using a tape-casting technique. However, many difficulties have appeared in the engineering of such membranes such as high-temperature sealing. For tubular membranes, which are normally prepared by a paste-extrusion or isostatic-pressing, the sealing difficulty can be easily solved by keeping the sealing part outside of the high-temperature zone; this ensures that the temperature of the sealing part is reasonably low in order to obtain an excellent seal. However, a tubular membrane usually has a small packing density (defined as the membrane area per membrane tank volume) due to its relatively thick wall and large diameter. To avoid issues of small packing density and sealing difficulty, hollow fiber membranes are fabricated via a phase-inversion spinning/sintering technique and are currently the most popular architecture for engineering applications. Membrane reactor design, performance, and applications related to the utilization of natural gas (e.g., the partial oxidation of methane (POM)) and biofuels (e.g., ethanol oxidative steam reforming), and the treatment of greenhouse gases (e.g., thermal decomposition of carbon dioxide (TDCD)) are presented. A ceramic membrane cannot support itself when it is very thin (i.e., less than 500μm). A supported membrane (or asymmetric membrane), which comprises a thin, dense separation layer fabricated on a mechanically strong porous support layer, is considered to be a promising membrane geometry to enhance the oxygen flux without sacrificing mechanical strength.

Jin et al. and Dong et al. proposed a co-sintering technique to prepare asymmetric membranes with an ultra-thin separation layer. In this technique, a precursor of the separation layer was coated onto a green support by means of spin-coating or co-pressing with a substrate powder material using a uniaxial press. After high temperature sintering, an asymmetric membrane was formed (34,35). Liu et al. (36) recently reported a $SrCo_{0.4}Fe_{0.5}Zr_{0.1}O_{3-\delta}$ (SCFZ) asymmetric tubular membrane that was fabricated by means of a co-sintering technique. A green tubular SCFZ support was coated with an SCFZ precursor using a spin-spray technique. After sintering, a 20 μm dense layer was obtained. Compared to planar or tubular membranes, hollow fiber membranes have much greater packing density (the diameter of a single membrane is less than 1 mm) and thin separating dense layer (less than 50 μm); they also integrate different types of porous layers (i.e. finger-like layers and sponge-like layers). This structure provides a much larger gas/membrane interface and lower mass-transfer resistance and leads to an enhancement of surface exchange and permeation rates. However, the greatest disadvantage of single-channel HF membranes is their low mechanical strength, which is due to the low mechanical strength of the supporting porous layer. This disadvantage restricts the use of such membranes in further industrial applications. Zhu et al. (38) developed a multichannel hollow fiber (MCHF) membrane using $SrFe_{0.8}Nb_{0.2}O_{3-\delta}$and Nb_2O_5-doped $SrCo_{0.8}Fe_{0.2}O_{3-\delta}$ (SCFNb).This membrane is considered to be a promising architecture for CMRs.

A membrane naturally separates a reactor into two chambers and some of the species involved can selectively permeate through the membrane. Thus, the major functions of a dense membrane in a dense CMR can be classified into three categories. First, the membrane acts as a distributor for one of the reactants. Given the high oxygen flux (and perm selectivity) of a perovskite-type membrane, reactions can take place at the oxygen permeation side of the membrane. The dosing of oxygen can be easily and precisely controlled, which lowers the risk of thermal runaway in the case of an exothermic reaction. In addition, a better yield of intermediate oxidation products can be obtained because such reactors can work with a lower partial pressure of oxygen. Typical examples that can benefit from this are partial oxidation of hydrocarbons, oxidative coupling of hydrocarbons and oxidative dehydrogenation of hydrocarbons. The second major function of a membrane in a CMR is to selectively remove a species. This is important as it involves shifting a chemically equilibrated reaction in a desired direction by selectively removing one of the in-situ products from the reaction side of the membrane. Typical reactions that benefit from this function include hydrogen production and the decomposition of oxygen-containing compounds. The third major function involves coupling reactions. A CMR comprises two chambers separated by a membrane. Reactions can take place on both sides of the membrane, which makes it possible to couple multiple reactions in a CMR. In a coupling CMR, the product of a reaction on one side of the membrane, which permeates the membrane, can be the reactant for a second reaction on the other side of the membrane. In this way, the conversions of both reactions can be enhanced. Furthermore, an auto-thermal reactor can be constructed by coupling endothermic and exothermic reactions in a CMR. A typical case is the coupling decomposition of oxygen-containing gases (CO_2, N_2O, and H_2O) with a POM reaction.

Equation 4 is the most promising process for methane (CH_4) conversion (POM partial oxidation of methane) because it is a mild exothermic reaction with high selectivity and a desirable hydrogen/carbon monoxide (H_2/CO) ratio of 2:1.

$$CH_4 + ½\ O_2 \rightarrow 2H_2 + CO\ \Delta H^0_{298} = -35.7 kJ\ mol^{-1} \quad (4)$$

In this process, air is supplied to one side of the membrane and methane is supplied to the other side of the membrane. A dual-layer configuration was designed. The dense layer was made of 0.5 wt% SCFNb, which has a high oxygen permeability, and the porous layer is made of $Sr_{0.7}Ba_{0.3}Fe_{0.9}Mo_{0.1}O_{3-\delta}$ (SBFM), which shows an excellent reduction tolerance (e.g. in hydrogen).This dual-layer membrane reactor design keeps the reaction site away from the surface of the dense layer and can be operated steadily for more than 1500 h with no significant performance degradation. CO selectivity =98%,H_2 production =45ml.cm^{-2}min^{-1}, methane conversion =80%, oxygen permeation flux=13ml.cm^{-2}min^{-1}, H_2/CO ratio =2 (25).

The thermal decomposition of carbon dioxide (TDCD) into carbon monoxide and oxygen is considered to be a potential route for carbon dioxide capture and utilization. However, carbon dioxide decomposition is limited by its thermodynamic equilibrium. To achieve a high conversion, high-density energy inputs such as a very high temperature (> 1727°C) are necessary in a fixed-bed reactor. Integrating the TDCD and POM reactions in a dense CMR shows a remarkable advancement in the utilization of carbon dioxide to supply oxygen for the POM reaction. A dense CMR based on a disk-like SCFZ membrane was designed for the coupling of the TDCD and POM reactions. The TDCD reactions take place on one side of the membrane in the presence of a supported palladium (Pd)-based catalyst, and methane reacts with oxygen (which permeates from the TDCD side) over a supported nickel (Ni)-based catalyst on the other side of the membrane. At 900°C, the carbon monoxide selectivity and carbon dioxide conversion reached 100% and 15.8%, respectively. Having the POM occur on the opposite side of the membrane to the TDCD can increase the driving force and promote carbon dioxide decomposition (25).

A triple-layer composite structure (porous/dense/porous) for the TDCD and POM coupling reaction was proposed . SBFM and $La_{0.8}Sr_{0.2}MnO_{3-\delta}$ yttria-stabilized zirconia (LSM-YSZ) were fabricated as porous layers on the dense SCFNb membrane, and were closed to the POM and TDCD sides, respectively. The functions of reduction resistance, carbon dioxide resistance, and high permeability were assigned to the SBFM, LSM-YSZ, and SCFNb layers, respectively. The essence of this design is that each of the layers plays its respective function and synergistically contributes to improve the stability and conversion. This novel reactor attained a 20.58% carbon dioxide conversion at 900°C, and could be steadily operated for more than 500 h (25).

Challenges: In addition to membrane reactor design, many technological gaps remain to be filled for the successful application of dense CMRs on industrial scales. These include high-temperature sealing and operation lifetime. Most of these materials operate at a high temperature, normally higher than 700°C, in order to obtain the desired oxygen flux. One effective solution is to lower operation temperature, resulting in a lower requirement for sealing and better stability. Furthermore, the commercialization and industrialization processes of perovskite membranes strongly rely on the large-scale fabrication method.

It is commonly accepted that the metal elements of the A or B site of the typical ABO_3 structure, along with their stoichiometric coefficients, are significant in determining the properties of perovskite-type oxides. In 2016, Zhu et al. (39) reported a new route for designing membrane materials for low-temperature permeation by the rational doping of fluorion (F^-) in a perovskite oxide. The doped fluorion reduced the valence electron density of the oxygen ion and hence weakened the B–O–B chemical bonds, thereby creating a fast O_{2-} transport path and facilitating oxygen permeation. The oxygen flux of fluorion-doped $SrCo_{0.9}Nb_{0.1}O_{3-\delta}F_{0.1}$ (SCNF) and $Ba_{0.5}Sr_{0.5}Co_{0.8}Fe_{0.2}O_{3-\delta}F_{0.1}$ (BSCFF) perovskiteoxyfluoride membranes was more than two and three times greater, respectively, than those of undoped $SrCo_{0.9}Nb_{0.1}O_{3-\delta}$ (SCN) and $Ba_{0.5}Sr_{0.5}Co_{0.8}Fe_{0.2}O_{3-\delta}$ (BSCF) membranes at 600°C. The typical fabrication procedure of perovskitehollow fibers comprises the following steps: ①the high-temperature synthesis of perovskite powder (usually > 700°C) via solid-state reaction or a wet chemistry route; ②phase inversion to spin the HF precursor; and ③high-temperature sintering. These processes are labor-, energy-, and time-consuming as well as environmentally unfriendly. In addition, it is usually impossible to precisely control theca ion stoichiometry of the perovskite oxides. Thus, simple and reliable fabrication remains a major challenge.

Porous ceramic membrane reactors: Two main configurations of porous CMRs for heterogeneous catalysis are commonly discussed in the literature: side-stream and submerged configurations (40-44). In the side-stream configuration, the reactions occur in a reaction vessel (which is usually stirred) and product separation is performed in a cross flow membrane filtration unit that is placed outside of the reaction vessel. The reaction zone and separation zone are segregated by the membrane, which benefits membrane replacement, cleaning, and scaling up, and which permits more flexibility. However, in the side-stream configuration, significant catalyst loss can occur in the surfaces or pores of the membrane, the pipe work, and the pumping system. In addition, the use of a recirculation loop increases the energy cost. In contrast, in the submerged configuration, the membrane is located in the reaction vessel, where it is submerged under the liquid and the permeate is removed using a pump or gravity. Thus, a major advantage of the submerged configuration is that the catalyst loss and energy consumption are much less than in the side-stream configuration.

Zhong et al.(45) and Chen et al. (46) studied the hydrogenation of p-nitro phenol to p-aminophenol over nickel nanoparticles in a membrane reactor using the side-stream and submerged configurations, respectively. A much more stable reaction rate over time was observed in the submerged configuration, and it was noted that a lower surface area in the recirculating loop and a high flow rate favored the suppression of the membrane-fouling from adhesion of nickel nanoparticles. However, the membrane area per reactor volume is restricted due to the limited reactor volume. From this point of view, the side-stream configuration is beneficial in some circumstances for scaling up.

Classic configurations of a porous CMR are

- Side-stream configuration
- Submerged configuration
- Dual-membrane configuration

A membrane reactor that combines the reactant distribution with catalyst separation is expected to enhance the product selectivity and yield. Two porous ceramic tubular membranes were employed in this design, with one acting as a reactant distributor controlling the supply of the reactants and the other acting as a membrane separator for the in situ separation of catalysts from the products (47). Figure 12 illustrates the dual-membrane configuration. The performance of phenol hydroxylation with hydrogen peroxide (H_2O_2) over a titanium silicalite-1 (TS-1) catalyst in the dual-membrane reactor was evaluated (47). Compared with traditional H_2O_2 feeding modes, the dual-membrane configuration provides a higherdihydroxybenzene selectivity and a catalyst rejection rate of almost 100%. This study demonstrated the advantages of the dual-membrane reactor in enhancing reaction selectivity, product separation, and catalyst separation simultaneously in a continuous heterogeneous catalytic reactor.

In a membrane reactor design, combining the existing reactor with a commercial membrane with minimum modification would be the most effective strategy. However, commercial membranes may not meet the individual requirements of the application objects. Therefore, membranes must be designed and optimized for individual application, which is the concept behind application-oriented ceramic membrane design. Considering the diverse sizes of the catalysts that are used in different applications, the separation efficiency and thus the CMR performance largely depend on the membrane microstructures, which include pore size and pore-size distribution, porosity, and thickness. Heterogeneous catalysis based on ultrafine catalysts and heterogeneous catalysis based on nano-sized catalysts are taken as model systems in order to illustrate CMR design from a performance-microstructure perspective.

CMR design for Ultrafine catalysts: The use of the TS-1 catalyst, which has a high catalytic activity and selectivity, has attracted extensive attention. In general, the particle size of TS-1 is 0.1–0.3 μm, which is too fine for effective removal from the reaction slurry by either gravity settling or porous tube filtration. Tubular membranes are commonly used in porous CMRs due to their high mechanical strength, and these membranes are commonly applied in TS-1 separation. The small pore size of the HF membrane facilitated the generation of droplets on the microscale. In contrast to the drop-by-drop mode (in which a reagent is added dropwise) and the one-lot mode (in which a reagent is added all at once), the hydrogen peroxide reactant was distributed by a ceramic HF membrane with a reduced membrane pore size (2.0–0.3 μm), resulting in significant enhancement of the dihydroxybenzene selectivity.

CMR design for nano-catalysts: Compared with catalysts that are based on bulk materials, a nano-sized catalyst often exhibits superior catalytic properties. However, the high surface energy causes nano-sized catalysts to be easily adsorbed onto the components of the system during catalyst recovery. It has been demonstrated that porous ceramic membranes can completely remove nano-sized nickel catalysts (60 nm) from a reaction slurry (48). However, the loss of nanosized nickel particles in the slurry and the formation of caking on the membrane surface cause a degradation of the permeation flux. Chen et al. (49) developed an improved fabrication technique to enhance the adhesion of metal particles, such as palladium (Pd), to the membrane surface by silanizing the membrane with γ-aminopropyltriethoxysilane. A more uniform distribution of Pd nanoparticles and a smaller particle size were obtained. The research group then proposed a flow-through method (49-51)to increase the loading amount of Pd. Pd nanoparticles can be deposited not only on the membrane surface, but also in the membrane pores, by letting the solution flow through the membrane. The combination of both surface silanization and the flow-through method resulted in a significant improvement of the catalytic reduction of p-nitrophenol to p-aminophenol, compared with the traditional impregnation method(49-51). As a support, hollow fiber(HF) ceramic membranes can provide more surface area per unit of volume and can significantly cause reduction in the deposition of nano-sized particles. The hydrogenation rate of an HF CMR loaded with Pd is at least 44% higher than that of a tubular CMR loaded with Pd.

Challenges affecting porous CMRs

- Membrane reactor design. The major drawback of the sidestream configuration is the adsorption of catalyst in the loop, whereas the submerged configuration has many advantages that include a small footprint, reduced catalyst adsorption, and significantly reduced energy consumption. Better performance was obtained in a dual-membrane reactor, which introduces an additional membrane distributor, due to good distribution of the reactants. Combining a dual-membrane reactor with an airlift membrane reactor provides another opportunity in gas–liquid heterogeneous catalysis by improving the gas–liquid mass transfer.
- Engineering the membrane: Tubular membranes are commonly used and studied for use in porous CMRs. However, their relatively large diameter and thick wall result in low surfacearea- to-volume ratios and large mass-transfer resistance, and hence in a low separation efficiency for the entire membrane system.Hollow Fiber membranes appear to overcome these limitations. For practical application, an appropriate pore size and distribution are essential in order to generate uniform droplets on the microscale. Because of the large surface-area-to-volume ratio of HF membranes, they can support nano-sized catalysts.
- Process simulation: Most CFD models consider the catalytic reaction and the membrane separation process separately. Therefore, integrally linking the two processes is essential in establishing CFD models that help us to understand the process in a way that is close to reality.

Commercializations: Some successful industrial applications of porous CMRs have been achieved. A side-stream membrane reactor was designed in Zhejiang province, China, for cyclohexanoneammoximation over TS-1. The membrane model consists of 241 tubular porous ceramic membranes through which the catalyst can be retained and recycled. Less than 1 mgL^{-1} of catalyst was found in the permeation, and the

conversion and selectivity were higher than 99.5%. The greatest advantage of a ceramic membrane is that it can be easily cleaned using strong basic and acidic solutions. Another industrial application of a porous CMR has been achieved for p-aminophenol production. A microfiltration membrane based on a porous ceramic membrane (from Jiangsu Jiuwu Hi-Tech Co., Ltd.) was successfully employed to recover nanosized catalysts. This project yields a p-aminophenol production of 30000 ton per annum in Anhui province, China.

*Zeolite membrane reactor:*In reported literature (60), a supported β-zeolite membrane reactor was used for the reaction of benzene with propylene to form cumene, between 200 to 300°C. *β*-zeolite was prepared by hydrothermal synthesis using silica, aluminum metal and Tetraethylammonium hydroxide(35%) as precursors. Flow through membrane reactor provided highest conversion of 42.9% at 200°C with cumene selectivity of 43.48%. This selectivity was constant during a continuous24 h evaluation of each reaction temperature in the 200 °C to 300 °C range.

Summary

While there are numerous reviews about membrane-based separations (56,57,58), there is not much information collated about enhanced separations involving chemical reactions (52). Hence, the intention of this paper was to fill the knowledge gap. Polymeric membranes can serve as materials for degradation of carcinogenic compounds in water sources, as an integral part of lithium-oxygen battery cells and extensively in pervaporation applications to break azeotropic mixtures.Metallic membrane reactors aid in gas phase reactions. Ceramic Membrane Reactorsnot only integrate various membrane operations simply into one unit; they also intensify the process by operating in a synergistic fashion. Examples of reactions that benefit from dense CMRs include the partial oxidation of methane to syngas, steam reforming to produce hydrogen, and the thermal decomposition of carbon dioxide.

Examples of reactions that benefit from porous CMRs include the heterogeneous catalysis of phenol hydroxylation with hydrogen peroxide or oxygen, cyclohexanoneammoximation, and the hydrogenation of p-nitrophenol to p-aminophenol. Thus, this paper provided a review of simultaneous chemical reaction and membrane separations. Membrane reactors can enhance conversion in chemical reaction processes and lower cost. With increasing awareness about membranes to make industrial processes (small, medium) more efficient and more economical, there is potential for researchers to convert membrane reactors from thin films to tubular form and employ them for real-time processes as evidenced in this paper. Some challenges remain such as membrane fabrication for large scale processes, accuracy and reproducibility of fabrication techniques and sealing the membranes into modules for large scale processes.

Acknowledgements

The first author would like to thank the IICT-RMIT Ph.D. program for this opportunity and funding.

REFERENCES

1. Scott R. Lewis, SauravDatta, MinghuiGui, Eric L. Coker, Frank E. Huggins, Sylvia Daunert, Leonidas Bachas, and Dibakar Bhattacharyya, Reactive nanostructured membranes for water purification, PNAS , May 24, 2011 ,vol. 108 , no. 21 , 8577–8582.
2. Garcia Villaluenga, J.P. A. Tabe-Mohammadi, 2000. A review on the separation of benzene/cyclohexane mixtures by pervaporation processes, Journal of Membrane Science 169 159–174.
3. Hyun-Sik Woo, Jae-Hong Kim, Yong-Bok Moon, Won Keun Kim, Kyoung Han Ryu,Dong-Won Kim, 2018. A dual membrane composed of composite polymer membrane and glass fiber membrane for rechargeable lithium-oxygen batteries, Journal of Membrane Science 550 340–347
4. Sreenivasa Reddy Puniredd, SeahWeiyi, M.P. Srinivasan, Pd–Pt and Fe–Ni nanoparticles formed by covalent molecular assembly in supercritical carbon dioxide, Journal of Colloid and Interface Science 320 (2008) 333–340.
5. ZheXu, Li Wang, Cunming Yu, Kan Li, Ye Tian, and Lei Jiang, 2018. In Situ Separation of Chemical Reaction Systems Based on a Special Wettable PTFE Membrane, Adv. Funct. Mater., 28, 1703970.
6. Francesco Galiano, Roberto Castro-Muñoz, Raffaella Mancuso, Bartolo Gabriele and Alberto Figoli, 2019. Membrane Technology in Catalytic Carbonylation Reactions, Catalysts, 9(7), 614.
7. De Souza Figueiredo, K.C., Salim, V.M.M., Borges, C.P. Synthesis and characterization of a catalytic membrane for pervaporation-assisted esterification reactors. Catal. Today 2008, 133, 809–814.
8. Zhang, W., Qing, W., Chen, N., Ren, Z., Chen, J., Sun, W. Enhancement of esterification conversion using novel composite catalytically active pervaporation membranes. J. Membr. Sci. 2014, 451, 285–292
9. El-Zanati, E., Abdallah, H. 2015. Esterification of ethyl hexanoic acid using flow-through catalytic membrane reactor. Catal. Ind. 7, 91–97.
10. Bagnato, G., Figoli, A., Ursino, C., Galiano, F., Sanna, A. 2018. A novel Ru-polyethersulfone (PES) catalytic membrane for highly efficient and selective hydrogenation of furfural to furfuryl alcohol. J. Mater. Chem. A , 6, 4955–4965.
11. Schmidt, A., Haidar, R., Schomäcker, R. 2005. Selectivity of partial hydrogenation reactions performed in a pore-through-flow catalytic membrane reactor. Catal. Today , 104, 305–312.
12. Cruz-López, A., Guilhaume, N., Miachon, S., Dalmon, J.A. Selective oxidation of butane to maleic anhydride in a catalytic membrane reactor adapted to rich butane feed. Catal. Today 2005, 107, 949–956
13. Kniep, J., Lin, Y.S. 2011. Partial oxidation of methane and oxygen permeation in SrCoFeOx membrane reactor with different catalysts. *Ind. Eng. Chem. Res.*, 50, 7941–7948.
14. Li, C.F., Zhong, S.H. 2003. Study on application of membrane reactor in direct synthesis DMC from CO_2 and CH_3OH over Cu-KF/MgSiO catalyst. Catal. Today 82, 83–90.
15. Yamanaka, I., Funakawa, A., Otsuka, K., 2004. Electrocatalytic synthesis of DMC over the Pd/VGCF membrane anode by gas-liquid-solid phase-boundary electrolysis. *J. Catal.*, *221*, 110–118.

16. Baker, R.W., Wijmans, J.G., Huang, Y. 2010. Permeability, permeance and selectivity: A preferred way of reporting pervaporation performance data. *J. Membr. Sci.,* 348, 346–352
17. Wei, H., Wang, F., Zhang, J., Liao, B., Zhao, N., Xiao, F., Wei, W., Sun, Y. Design and control of dimethyl carbonate—Methanol separation via pressure-swing distillation. Ind. Eng. Chem. Res. 2013, 52, 11463–11478
18. Won, W., Feng, X., Lawless, D. 2002. Pervaporation with chitosan membranes: Separation of dimethyl carbonate/methanol/water mixtures. *J. Membr. Sci.,* 209, 493–508.
19. Won, W., Feng, X., Lawless, D. 2003. Separation of dimethyl carbonate/methanol/water mixtures by pervaporation using crosslinked chitosan membranes. Sep. *Purif. Technol*. 31, 129–140.
20. Wang, L., Li, J., Lin, Y., Chen, C. 2007. Separation of dimethyl carbonate/methanol mixtures by pervaporation with poly (acrylic acid)/poly (vinyl alcohol) blend membranes. *J. Membr. Sci.*, *305*, 238–246.
21. Wang, L., Li, J., Lin, Y., Chen, C. 2009. Crosslinked poly (vinyl alcohol) membranes for separation of dimethyl carbonate/methanol mixtures by pervaporation. *Chem. Eng. J.,* 146, 71–78.
22. Dong, E., Lin, Y. 2013. Synthesis of an organophilic ZIF-71 membrane for pervaporation solvent separation. *Chem. Commun.,* 49, 1196–1198.
23. Yi-Ming Sun and Soon-Jai Khang, 1988. Catalytic Membrane for Simultaneous Chemical Reaction and Separation Applied to a Dehydrogenation Reaction, Ind. *Eng. Chem. Res.,* 27, 1136-1142
24. Kyung-Ran Hwang, Sung-Wook Lee, Dong-Wook Lee, Chun-Boo Lee, Sung-MiJi, Jong-Soo Park, 2014. Bi-functional hydrogen membrane for simultaneous chemical reaction and hydrogen separation, International journal of hydrogen energy 39 2614-2620.
25. Guangru Zhang, Wanqin Jin, Nanping Xu, 2018. Design and Fabrication of Ceramic Catalytic Membrane Reactors for Green Chemical Engineering Applications, Engineering 4 848–860.
26. Dixon AG. 2003. Recent research in catalytic inorganic membrane reactors. *Int. J.Chem React Eng*., 1(1):R6
27. Sanchez Marcano JG, Tsotsis TT. Catalytic membranes and membrane reactors. Weinheim: Wiley-VCH Verlag GmbH & Co. KGaA; 2004.
28. Thursfield A., Murugan A., Franca R., Metcalfe IS. 2012. Chemical looping and oxygen permeable ceramic membranes for hydrogen production—a review. *Energy Environ Sci.*, 5(6):7421–59.
29. Dong X., Jin W., Xu N., Li K. 2011. Dense ceramic catalytic membranes and membrane reactors for energy and environmental applications. Chem Commun (Camb) 47(39):10886–902.
30. Bouwmeester HJM. Dense ceramic membranes for methane conversion. Catal. Today 2003;82(1–4):141–50.
31. Yang W, Wang H, Zhu X, Lin L. 2005. Development and application of oxygen permeable membrane in selective oxidation of light alkanes. *Top Catalysis*., 35(1–2):155–67.
32. Liu Y, Tan X, Li K. 2006. Mixed conducting ceramics for catalytic membrane processing. *Catal Rev Sci Eng*., 48(2):145–98.
33. Wei Y., Yang W., Caro J., Wang H. 2013. Dense ceramic oxygen permeable membranesand catalytic membrane reactors. *Chem Eng J.,* 220:185–203.
34. Jin W, Li S, Huang P, Xu N, Shi J. 2001. Preparation of an asymmetric perovskite-type membrane and its oxygen permeability. *J Membr Sci.,*185(2):237–43.
35. Dong X., Zhang G., Liu Z., Zhong Z., Jin W., Xu N. 2009. CO2-tolerant mixed conducting oxide for catalytic membrane reactor. *J Membr Sci.,* 340(1–2):141–7.
36. Liu Z., Zhang G., Dong X., Jiang W., Jin W., Xu N. 2012. Fabrication of asymmetric tubular mixed-conducting dense membranes by a combined spin-spraying and co-sintering process. *J Membr Sci*., 415–416:313–9.
37. Wu Z., Hidayati Othman N., Zhang G., Liu Z. Jin W., Li K., 2013. Effects of fabrication processes on oxygen permeation of Nb_2O_5-doped $SrCo_{0.8}Fe_{0.2}O_{3-\delta}$microtubular membranes. *J Membr Sci.,* 442:1–7.
38. Zhu J, Dong Z, Liu Z, Zhang K, Zhang G, Jin W. 2014. Multichannel mixed-conductinghollow fiber membranes for oxygen separation. *A I Ch E Journal*., 60(6):1969–76.
39. Zhu J, Liu G, Liu Z, Chu Z, Jin W, Xu N. 2016. Unprecedented perovskiteoxyfluoride membranes with high-efficiency oxygen ion transport paths for low temperature oxygen permeation. Adv Mater 28(18):3511–5.
40. Zou Y, Jiang H, Liu Y, Gao H, Xing W, Chen R. 2016. Highly efficient synthesis of cumene via benzene isopropylation over nano-sized beta zeolite in a submerged ceramic membrane reactor. *Separ Purif Tech.,* 170:49–56.
41. Zou Y, Jiang H, Gao H, Chen R. 2016. Efficient recovery of ultrafine catalysts from oil/water/solid three-phase system by ceramic microfiltration membrane. *Korean J Chem Eng.,* 33(8):2453–9.
42. Jiang H, Jiang X, She F, Wang Y, Xing W, Chen R.2014. Insights into membrane fouling of a side-stream ceramic membrane reactor for phenol hydroxylation over ultrafine TS-1. *Chem Eng J.,* 239:373–80.
43. Mao H, Chen R, Xing W, Jin W. 2016. Organic solvent-free process for cyclohexanoneammoximation by a ceramic membrane distributor. *Chem Eng Technol.,* 39(5):883–90.
44. Jiang X, She F, Jiang H, Chen R, Xing W, Jin W. Continuous phenol hydroxylation over ultrafine TS-1 in a side-stream ceramic membrane reactor. Korean J ChemEng 2013;30(4):852–9.
45. Zhong Z, Xing W, Jin W, Xu N. 2007. Adhesion of nanosized nickel catalysts in the nanocatalysis/UF system. AIChE J., 53(5):1204–1210.
46. Chen R, Du Y, Wang Q, Xing W, Jin W, Xu N. 2009. Effect of catalyst morphology on the performance of submerged nanocatalysis/membrane filtration system. *Ind Eng Chem Res.,* 48(14):6600–7.
47. Jiang H, Meng L, Chen R, Jin W, Xing W, Xu N. 2011. A novel dual-membrane reactor for continuous heterogeneous oxidation catalysis. *Ind Eng Chem Res.,* 50 (18):10458–64.
48. Zhong Z, Li W, Xing W, Xu N. 2011. Crossflow filtration of nanosized catalysts suspension using ceramic membranes. *Separ Purif Tech*., 76(3):223–30.
49. Chen R, Jiang Y, Xing W, Jin W. 2011. Fabrication and catalytic properties of palladium nanoparticles deposited on a silanized asymmetric ceramic support. *Ind Eng Chem Res.,* 50(8):4405–11.
50. Chen R, Jiang Y, Xing W, Jin W. 2013. Preparation of palladium nanoparticles deposited on a silanized hollow fiber ceramic membrane support and their catalytic properties. *Ind EngChem Res.,* 52(14):5002–8.
51. Li H, Jiang H, Chen R, Wang Y, Xing W. 2013. Enhanced catalytic properties of palladium nanoparticles deposited

on a silanized ceramic membrane support with a flow-through method. *Ind Eng Chem Res*., 52(39):14099–106.
52. Handbook of membrane reactors, Volume 1: fundamental material science, design and optimization, Angelo Basile, Woodhead Publishing Series in Energy :Number 55, 2013.
53. Emma Palo, Annarita Salladini, Barbara Morico, Vincenzo Palma, Antonio Ricca and Gaetano Iaquaniello, 2018. Application of Pd-Based Membrane Reactors: An Industrial Perspective, Membranes, 8, 101; doi:10.3390/membranes8040101.
54. Scott, R.W. Datye, A.K. Crooks, R.M. 2003. J. Am. Chem. Soc. 125 3708.
55. H. Ye, R.M. Crooks, J. Am. Chem. Soc. 129 (2007) 3627.
56. Clem E. Powell, Greg G. Qiao, 2006. Polymeric CO2/N2 gas separation membranes for the capture of carbon dioxide from power plant flue gases, Journal of Membrane Science 279 1–49.
57. Richard W. Baker, 2010. Research needs in the membrane separation industry: Looking back, looking forward, Journal of Membrane Science 362 134–136.
58. Llyod M. Robeson, 2008. The upper bound revisted, Journal of Membrane Science 320 390–400.
59. Fane, A.G., Rong Wang, Mathew H. Xu, 2015. Synthetic membranes for water purification: status and future, Angew. *Chem. Int. Ed*., 54, 3368 – 3386.
60. Miguel Torres-Rodríguez, Mirella Gutiérrez-Arzaluz, Violeta Mugica-Álvarez, Julia Aguilar-Pliego and Sibele Pergher, 2012. Alkylation of Benzene with Propylene in a Flow-Through Membrane Reactor and Fixed-Bed Reactor: Preliminary Results, Materials, 5, 872-881; doi:10.3390/ma5050872.

****